8286 *Macromolecules* **2009**, *42*, 8286–8297
DOI: 10.1021/ma901453x

Macromolecules
ARTICLE

# Crystallization Properties and Polymorphic Behavior of Isotactic Poly(1-Butene) from Metallocene Catalysts: The Crystallization of Form I from the Melt

**Claudio De Rosa,*,† Finizia Auriemma,† Odda Ruiz de Ballesteros,† Fortunata Esposito,† Domenico Laguzza,† Rocco Di Girolamo,† and Luigi Resconi‡,§**

†*Dipartimento di Chimica "Paolo Corradini", Università di Napoli "Federico II", Complesso Monte S. Angelo, Via Cintia, I-80126 Napoli, Italy, and* ‡*Basell Polyolefins, Centro Ricerche G. Natta, P. le G. Donegani 12, I-44100 Ferrara, Italy.* §*Present address: Borealis Polyolefine GmbH, St. Peter Strasse 25, 4021 Linz, Austria.*

*Received July 7, 2009; Revised Manuscript Received September 6, 2009*

ABSTRACT: A study of the crystallization from the melt and of the polymorphic behavior of isotactic poly(1-butene) (iPB) prepared with metallocene catalysts is presented. Samples of isotactic polybutene of different stereoregularity, containing different concentrations of stereodefects (*rr* triads defects) and regiodefects (4,1 units) have been prepared with different $C_2$- and $C_1$-symmetric metallocene catalysts. The concentration of defects and the molecular mass are controlled through a rational choice of the catalyst structure and conditions of polymerization. Highly isotactic samples with concentration of *rr* stereodefects lower than 2 mol %, crystallize from the melt in the metastable form II. This is a common polymorphic behavior observed in iPB samples prepared with Ziegler−Natta catalysts and extensively reported in the literature. More stereodefective iPB samples, containing concentration of stereodefects higher than 2 mol %, crystallize form the melt as mixtures of form II and form I, the fraction of crystals of form I increases with increasing concentration of defects and decreasing cooling rate from the melt, and samples with concentration of *rr* defects of 3−4 mol % crystallize from the melt in the pure form I at low cooling rates. This is the first experimental observation of the crystallization of the stable trigonal form I of iPB from the melt at atmospheric pressure. This result may be of interest because the crystallization of the metastable form II from the melt and the spontaneous transformation at room temperature of form II into the stable form I has been considered for long time an unavoidable problem that stands in the way of the industrial development of the Ziegler−Natta iPB.

## Introduction

Isotactic poly(1-butene) (iPB) was first synthesized with Ziegler−Natta catalysts,[1] and it showed interesting physical and mechanical properties but also complex polymorphic behavior that has limited its commercial development. iPB crystallizes in three different polymorphic forms, defined forms I, II, and III, which differ for the chain conformations and the packing of chains.[2−14] Form I is the most stable form and is characterized by chains in $3_1$ helical conformation packed in a trigonal unit cell (space group $R3c$ or $R\bar{3}c$).[2,3] Form II has chains in $11_3$ helical conformation packed in a tetragonal unit cell (space group $P\bar{4}$).[4−7] In form III, chains with $4_1$ helical conformation are packed in an orthorhombic unit cell (space group $P2_12_12_1$).[8−10]

The conditions of crystallization of the various forms have been investigated in great detail,[11−21] mainly on iPB samples prepared with Ziegler−Natta catalysts. The tetragonal form II is the kinetically favored modification of iPB and is generally obtained by melt crystallization.[4,6,15−21] Form II transforms into the most stable form I on storage at room temperature.[2,11,15−26] Form III is generally obtained by crystallization form diluite solutions.[11−13]

Form I exists actually in two variants, defined forms I and I′, depending on the way it is produced. Form I refers usually to a crystal modification that is generated via a solid-state transformation of form II by aging at room temperature, whereas form I′ refers to the same trigonal crystal structure with chains in $3_1$ helical conformation obtained by direct crystallization from melt or solution.[12] The difference may not be trivial, since their melting temperatures have been reported to be significantly different.[12] The most stable form I melts at about 130 °C whereas form I′ melts at about 90−95 °C, even though they show the same crystal structure.[12] Because of this difference form I′ has been regarded to be an imperfect form I with many defects.[27] Forms II and III melt at temperatures of 124 and 106 °C, respectively,[11,12] lower than form I.

All three forms can be obtained by direct crystallization from solution (therefore we refer to forms I′, II and III) although the proportions of the various forms depend in a complex manner, not yet fully elucidated, on the crystallization conditions (solvent, and crystallization temperature) and annealing/melting of the suspension of crystals,[12,28,29] indicating that some kind of memory effect occurs in the solutions crystallization of iPB. Moreover, very thin films of all three forms (forms I′, II and III) have also been produced by epitaxial crystallization from the melt, by using appropriate substrates.[30,9,10]

Melt crystallization usually leads to the formation of only form II.[3,6−14] However, when iPB is melt-crystallized under high hydrostatic pressure (higher than about 1000 atm),[31,32] by a special melt-stretching technique,[18] by self-nucleation,[33] or in single crystals in ultrathin films at high crystallization temperatures,[34] or onto specific substrates for epitaxial growth,[30] formation of form I (actually form I′) has been reported. Formation of

*To whom correspondence should be addressed. Telephone: ++39 081 674346. Fax ++39 081 674090. E-mail: claudio.derosa@unina.it.

 Published on Web 10/02/2009 

**Table 1. Polymerization Temperatures ($T_p$), Intrinsic Viscosity [$\eta$], Average Molecular Masses ($\overline{M}_v$), Content of *mm*, *mr* and *rr* Triads, Concentration of Isotactic Pentad *mmmm*, Concentration of 4,1 Units, Total Concentration of Defect $\varepsilon$ (*rr* + 4,1), Melting Temperatures of Samples Crystallized from the Melt in Form II ($T_m$(II)) or in Form I′ ($T_m$(I′)) and of Crystals of Form I in Samples Melt-Crystallized and Aged at Room Temperature for a Long Time ($T_m$(I)), for Samples of Isotactic Poly(1-butene) Prepared With the Catalysts 1−10 of Chart 1**

| sample | catalyst | $T_p$ (°C) | [$\eta$] (dL/g) | $M_v$[a] | [*mmmm*] (%) | [*mm*] % | [*mr*] % | [*rr*] % | 4,1 (%) | $\varepsilon$ (%) | $T_m$ (II)[b] (°C) | $T_m$ (I′)[b] (°C) | $T_m$ (I)[c] (°C) |
|---|---|---|---|---|---|---|---|---|---|---|---|---|---|
| iPB1 | **1** | 70 | 1.43 | 243 300 | 100 | 100 | 0 | 0 | 0.3 | 0.3 | 110.3 | | 124.0 |
| iPB2 | **2** | 70 | 0.99 | 146 500 | 93.5 | 98.96 | 0.70 | 0.34 | 0.96 | 1.30 | 92.0 | | 112.0 |
| iPB10 | **10** | 70 | 1.26 | 204 000 | 98 | 98.85 | 0.77 | 0.38 | 0 | 0.38 | 110.0 | | 125.0 |
| iPB6a | **6** | 70 | 1.95 | 373 200 | 95.8 | 97.5 | 1.7 | 0.8 | 0 | 0.8 | 106.0 | | 123.7 |
| iPB6b | **6** | 70 | 1.37 | 229 300 | 96.2 | 97.7 | 1.5 | 0.8 | 0 | 0.8 | 104.7 | | 120.0 |
| iPB6c | **6** | 70 | 1.09 | 167 300 | 96.0 | 97.6 | 1.6 | 0.8 | 0 | 0.8 | 103.6 | | 123.0 |
| iPB6d | **6** | 70 | 0.59 | 72 000 | 96.0 | 97.6 | 1.6 | 0.8 | 0 | 0.8 | 103.4 | | 118.9 |
| iPB8 | **8** | 70 | 1.43 | 243 300 | 94.2 | 96.5 | 2.3 | 1.2 | 0 | 1.2 | 100.2 | | 115.0 |
| iPB7 | **7** | 70 | 1.75 | 321 400 | 92.2 | 95.7 | 2.9 | 1.4 | 0 | 1.4 | 95.5 | | 112.5 |
| iPB5 | **5** | 70 | 1.19 | 188 800 | 87.7 | 92.4 | 5 | 2.5 | 0 | 2.5 | 84.0 | 92 | 103.0 |
| iPB4a | **4** | 60 | 1.88 | 354 800 | 86.6 | 91.7 | 5.5 | 2.8 | 0 | 2.8 | 76.0 | 85 | 102.0 |
| iPB4b | **4** | 70 | 1.34 | 222 400 | 85.4 | 90.9 | 6.0 | 3.0 | 0 | 3.0 | 75.7 | 84.6 | 94.3 |
| iPB4c | **4** | 70 | 1.08 | 165 200 | 86.5 | 91.6 | 5.6 | 2.8 | 0 | 2.8 | 77.2 | 85 | 95.7 |
| iPB4d | **4** | 80 | 0.93 | 134 400 | 86.5 | 91.6 | 5.6 | 2.8 | 0 | 2.8 | | 77−86 | 98.6 |
| iPB3 | **3** | 70 | 0.92 | 132 400 | 77.7 | 86 | 9.4 | 4.7 | 0 | 4.7 | 68.0 | 83.6 | 92.0 |
| iPB9 | **9** | 70 | 1.31 | 215 600 | 76.1 | 84.9 | 10.1 | 5.0 | 0 | 5.0 | 65.0 | 71.0 | |

[a] From the values of intrinsic viscosity. [b] Melting temperatures of samples crystallized from the melt by cooling the melt to room temperature at 10 °C/min, measured from DSC scans at heating rate of 10 °C/min. The melting temperatures of melt-crystallized samples correspond to the melting of crystals of form II for samples with [*rr*] < 2 mol %, and to the melting of mixtures of crystals of form II and form I′ obtained directly from the melt for samples with [*rr*] > 2 mol %. [c] Melting temperature measured from DSC scans at heating rate of 10 °C/min of samples in form I obtained by spontaneous transformation of the form II (obtained by crystallization from the melt by cooling the melt to room temperature at 10 °C/min) by aging the melt-crystallized samples at room temperature for long time.

form III has also been reported when iPB is melt-crystallized with a specific nucleating agent.[9,30]

The usual crystallization from the melt of the metastable form II and the spontaneous transformation at room temperature of form II into form I are key features that have prevented the commercial diffusion of iPB notwithstanding the attractive physical properties. In fact, iPB exhibits advantages over other polyolefins, like polyethylene and polypropylene, in superior toughness, tear strength, flexibility, creep, and impact resistance and could find many applications in, for instance, pressurized tanks, tubes, and hot water pipes. However, the spontaneous solid phase transformation from form II into form I alters the physical properties. The material, indeed, becomes on aging more rigid with higher strength,[11,15,26,35,36] with an increase of melting temperature and density. Undesirable effects, such as shrinkage of the molded objects generated by densification, are generally observed. This phase transition requires several days to be completed at room temperature,[11,15,25,26,34−41] and longer times are required upon aging, both at lower and higher temperatures.[11,33] This slow kinetics has considerably limited the application of iPB, and a great deal of research has thus been oriented toward finding solutions to accelerate the transition.

It has been shown that, besides the aging temperature, molecular characteristics of the polymer, such as molecular weight,[13,17,25] degree of isotacticity,[17,25] and content of comonomer units,[5,25,42] also influence the rate of the phase transformation. It has also widely been reported that application of all kinds of mechanical stimuli, such as hydrostatic pressures,[33,34] shear or tensile stresses,[39,43−45] and addition of suitable substances[39,46−48] can remarkably increase the rate of transformation. The morphology of the as-crystallized form II also plays a role in the kinetics of transformation, and a faster conversion to form I has been observed in samples crystallized in form II at high temperatures.[35,37]

These studies have been performed only on iPB samples prepared with Ziegler−Natta catalysts. It is well-known that these heterogeneous catalysts lead to mixtures of macromolecules having different molecular weights, different stereoregularities, and different distributions of stereosequences, resulting in a nonuniform interchain composition of defects. The nonrandom distribution of defects (including comonomers) has prevented understanding the effects of the single type of defects (*stereo*- and *regio*-defects or comonomeric units) and of the molecular mass on the crystallization behavior of iPB and on the kinetics of form II−form I phase transition.

Recent extensive investigations of the structure of isotactic polypropylene (iPP) produced with metallocene catalysts have instead demonstrated the novel utility of single-center metallocene catalysts in understanding the correlations between chain microstructure and crystallization behavior of iPP.[49,50] Single-center metallocene catalysts, indeed, allow a perfect control over the chain microstructure, and polypropylene samples of any microstructure, characterized by different kinds and amounts of *regio*- and *stereo*-irregularities, have been produced.[51] In addition, metallocene catalysts may yield iPP samples and iPP-based copolymers[52] with a random defects distribution, uniform intermolecular distribution of the defect content, and narrow molecular weight distribution. The random distribution of defects has afforded opportunities for studying the influence of a single type of defect on the crystallization and physical properties of iPP and precise relationships between chain microstructure and polymorphic behavior have been found.[49,50,52]

Recently Resconi et al.[53] have studied the performance of both $C_2$- and $C_1$-symmetric zirconocenes of variable structure in the polymerization of liquid 1-butene in the polymerization temperature range 50−90 °C, and have demonstrated that the right choice of the metallocene catalyst can provide iPB with molecular masses covering the whole range of practical interest under industrially significant polymerization conditions, and having physical properties spanning a broader range than those of iPB samples from Ziegler−Natta catalysts. With some $C_1$-symmetric zirconocenes, average molecular masses approaching 400 000 have been obtained at a polymerization temperature of 70 °C, and at 90 °C the molecular mass remains above 150 000.[53] Moreover, the structure of the catalysts, precisely the substitution pattern of the indenyl part of the ligand can be modified in order to tune the polymer stereoregularity, from the value of the isotactic *mm* triad content of nearly 85% up to the high value of 99%. Some $C_2$-symmetric zirconocenes containing heterocycle based ligands have shown even higher isoselectivity, reaching *mm* triad content close to 100%, but are less regioselective, producing 0.2−0.3% of regiodefects represented by 4,1 units arising from secondary butene insertion and successive isomerization.[53]

**Chart 1. Structures of $C_2$-Symmetric (1 and 2) and $C_1$-Symmetric (3−10) Zirconocene Catalysts Used in the Butene Polymerization**

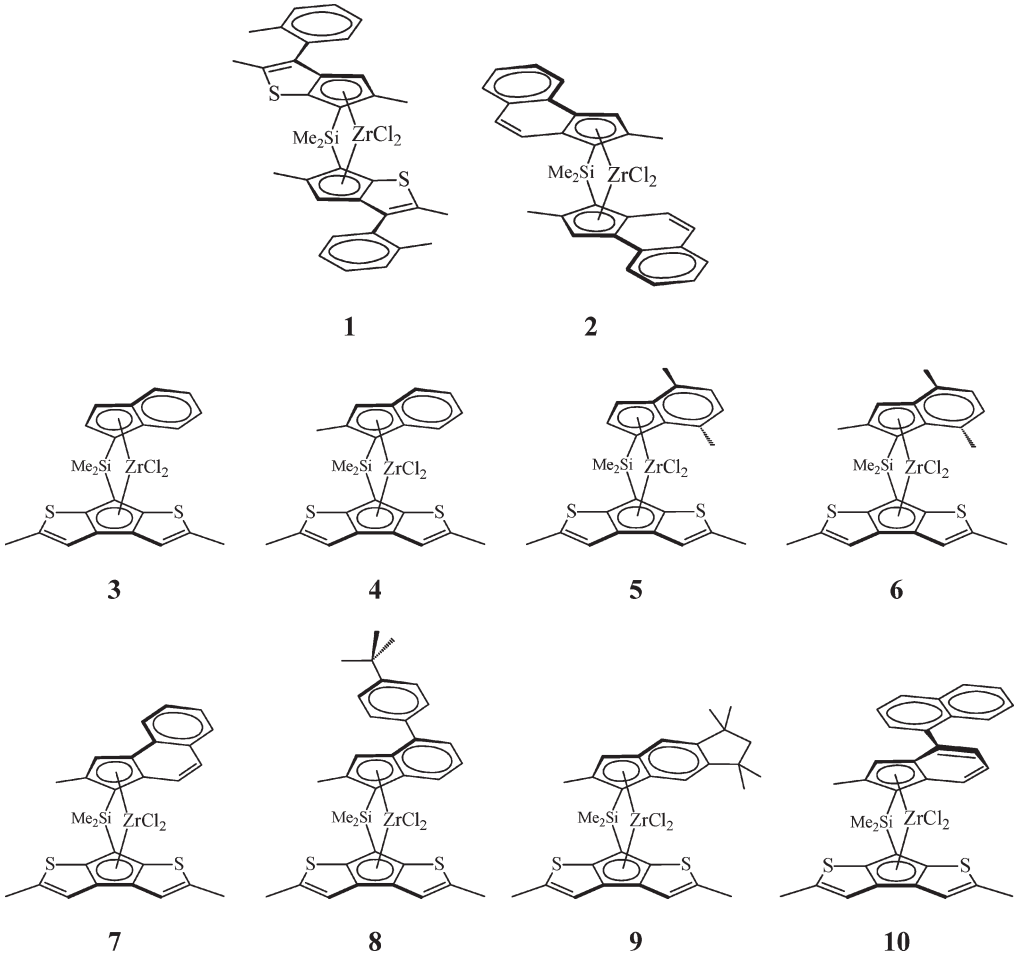


In this paper, we report a study of the polymorphic behavior of iPB samples of different stereoregularity prepared with the different metallocene catalysts described in ref 53. The samples are characterized by the presence of only one type of stereodefects (basically isolated *rr* triad defects) with concentration variable in a wide range, or regiodefects. These molecular features have allowed studying the effect of the presence of different types of microstructural defects (*stereo*- and *regio*-defects) on the crystallization from the melt of form II and form I of iPB.

## Experimental Section

Samples of iPB have been prepared in the laboratories of Basell Polyolefins (Ferrara, Italy) with different metallocene catalysts activated with methylalumoxane (MAO), as described in ref 53. All samples have been prepared in liquid 1-butene at polymerization temperature in the range 50−90 °C. Some samples have been prepared with two highly stereospecific, but not fully regiospecific $C_2$-symmetric catalysts **1** and **2** of Chart 1. These catalysts produce high molecular mass and highly stereoregular iPB samples containing very small concentrations of *rr* triad stereodefects and non negligible amount of regiodefects, represented by 4,1 units that are formed by a secondary (2,1) insertion of 1-butene followed by 2,1 → 4,1 isomerization.[53,54]

Other iPB samples have been prepared with the less stereospecific $C_1$-symmetric *ansa*-zirconocene catalysts **3**−**10**, shown in Chart 1. These complexes are based on the (substituted indenyl)-dimethylsilyl-[bis(2-methylthieno)cyclopentadienyl] ligand framework,[49,51b] and produce highly regioregular iPBs characterized by different stereoregularity, in particular different concentrations of *rr* triad stereodefects, depending on the indenyl substituents.[53] A list of the iPB samples is reported in Table 1.

The concentrations of the *mm*, *mr* and *rr* triads and of the isotactic pentad *mmmm* of all samples have been obtained from $^{13}C$ NMR analysis.

The intrinsic viscosity [$\eta$] was measured in tetrahydronaphthalene at 135 °C using standard Ubbelohde viscometer. The viscosity average molecular masses $M_v$ were determined from the intrinsic viscosity values according to the relationship $[\eta] = K(\overline{M}_v)^{\alpha}$, with $K = 1.78 \times 10^{-4}$ and $\alpha = 0.725$.[53]

The mass average molecular masses were evaluated from size exclusion cromatography (SEC). The SEC curves of all samples show narrow molecular weight distributions, with $M_w/M_n = 2-3$, typical of single-center metallocene catalysts.

The calorimetric measurements were performed with a differential scanning calorimeter (DSC), Perkin-Elmer DSC-7, calibrated with indium, in a flowing $N_2$ atmosphere. The melting temperatures of the samples were taken as the peak temperature of the DSC curves recorded at 10 °C/min.

X-ray powder diffraction profiles were obtained with Ni-filtered Cu K$\alpha$ radiation ($\lambda = 1.5418$ Å) with an automatic Philips diffractometer. The diffraction profiles at temperatures higher than the room temperatures have been collected with a Philips diffractometer provided with a TTK Anton-Paar camera.

The X-ray diffraction profiles in the ranges of $2\theta = 8-14°$ and $2\theta = 16-23°$ have been recorded during the isothermal crystallization from the melt at various crystallization temperatures in the TTK Anton-Paar camera. Each sample has been first heated at 180 °C and completely melted and the diffraction profile of the melt has been recorded at 180 °C. Then the samples have been rapidly cooled to the crystallization temperature $T_c$ and the

diffraction profiles have been recorded with continuous scans at collecting rate of 1.2 deg/min, every 5 min in the range $2\theta = 8-14°$, and 5.8 min in the range $2\theta = 16-23°$, up to the complete crystallization at $T_c$.

The fraction of crystals of form I with respect to the crystals of form II present in the melt crystallized samples ($f_I$) has been evaluated form the intensities of the $(110)_I$ reflection of form I at $2\theta = 9.9°$ and the $(200)_{II}$ reflection of form II at $2\theta = 11.9°$,[2,6] in the X-ray powder diffraction profiles of the melt-crystallized samples.

$$f_I = \frac{I(110)_I}{I(110)_I + RI(200)_{II}} 100$$

where $I(110)_I$ and $I(200)_{II}$ are the observed intensities of the $(110)_I$ reflection of form I at $2\theta = 9.9°$ and of the $(200)_{II}$ reflection of form II at $2\theta = 11.9°$, respectively, in the powder diffraction profile. The experimental intensities are corrected by the parameter $R$ that takes into account the different diffraction power of the $(110)_I$ and $(200)_{II}$ crystallographic planes in the trigonal and tetragonal crystal structures of form I and form II, respectively.

$$R = \frac{(|F(110)_I/N_I|)^2 Lp(110)_I}{(|F(200)_{II}/N_{II}|)^2 Lp(200)_{II}}$$

The parameter $R$ is the ratio between the square of the structure factors of the $(110)_I$ reflection of form I calculated in the space group $R3\bar{c}$,[2] and of the $(200)_{II}$ reflection of form II calculated in the space group $P\bar{4}$,[6] normalized for the total numbers of atoms present in the unit cells of form I ($N_I$) and form II ($N_{II}$) and multiplied for the respective multiplicities relative to powder diffraction, and, finally, corrected for the respective Lorentz−polarization factors $Lp$:

$$Lp = \frac{1 + \cos^2 2\theta}{\sin^2 \theta \cos \theta}$$

From the values of the structure factors a value of the parameter $R = 0.36$ has been calculated. The intensities of the $(110)_I$ and $(200)_{II}$ reflections have been evaluated by the area of the corresponding diffraction peaks in the powder diffraction profiles after subtraction of the amorphous contribution. The diffraction halo of the amorphous phase has been determined from the diffraction profile of a sample of atactic poly(1-butene) after suitable scaling.

## Results and Discussion

The metallocene catalysts of Chart 1 have allowed the synthesis of samples of iPB characterized by different concentration of *stereo-* and *regiodefects*. The iPB samples prepared with the $C_1$-symmetric complexes **3-10** are fully regioregular. The stereoregularity is tuned by modification of the substitution pattern of the indenyl part of the ligand, and the concentration of the isotactic *mm* triad changes from 85% up to 99%, with a single type of defect of stereoregularity represented by *rr* triads, which are randomly distributed along the polymer chains with a concentration in the range 0.3−5 mol % (Table 1). As in the case of propylene polymerization,[49,51] also in 1-butene polymerization with $C_1$-symmetric catalysts, the catalyst isoselectivity is practically independent of the polymerization temperature.

The $C_2$-symmetric zirconocenes turned out to be more isoselective than the $C_1$-symmetric catalysts,[53] producing iPB samples with *mm* triad content close to 100%, as in the case of the complex **1** (Table 1). These $C_2$-symmetric complexes are less regioselective, the most regular iPBs contain 0.2−0.3% of *regiodefects* represented by 4,1 units (Table 1) arising from secondary butene insertion followed by 2,1 → 4,1 isomerization.

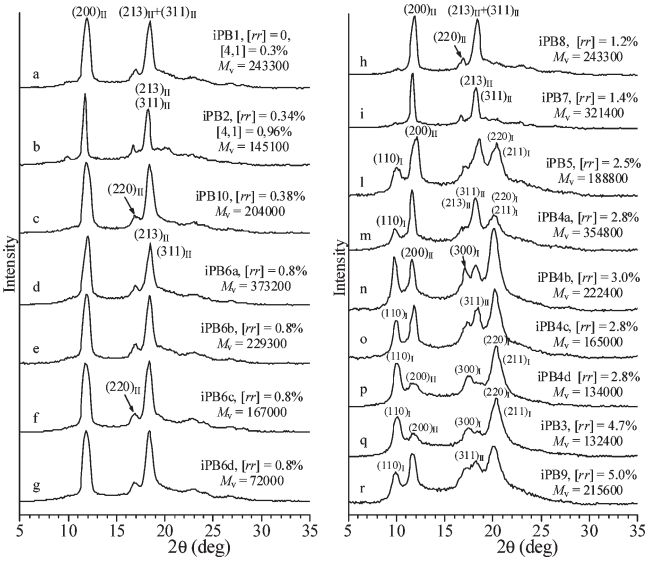


**Figure 1.** X-ray powder diffraction profiles of samples of iPB of different stereoregularity crystallized from the melt by cooling the melt to room temperature (or lower temperature) at cooling rate of 10 °C/min. The $(110)_I$, $(300)_I$ and $(220)_I + (211)_I$ reflections of form I at $2\theta = 9.9$, 17.3, and 20.5°, respectively, and the $(200)_{II}$, $(220)_{II}$ and $(213)_{II} + (311)_{II}$ reflections of form II at $2\theta = 11.9$, 16.9, and 18.3°, respectively, are indicated.

In the case of propylene polymerization, these highly isospecific $C_2$-symmetric catalysts allow occasional secondary (2,1) insertions of propylene.[51a] These secondary units do not affect catalyst activity, and are formed by enantioselective 2,1 insertions (that is insertion of the opposite enantioface of propylene with respect to primary enantioselective insertions) followed by a stereoregular primary insertion, thus generating erythro 2,1 units only. In the case of butene polymerization, these catalysts produce formation of $-(CH_2)_5-$ sequences that derive from a secondary (2,1) insertion of 1-butene followed by 2,1 → 4,1 isomerization.[53,54] These 4,1 units are actually the only observable regiodefects in iPB, secondary 2,1 units being undetectable, at least with the two MAO-activated $C_2$-symmetric zirconocenes **1** and **2**.[53]

The $C_2$-symmetric and $C_1$-symmetric metallocenes of Table 1 show a different hydrogen response.[53] Most of the catalysts are strongly activated by hydrogen addition during polymerization, due to the reactivation of sites bearing secondary chains, formed upon secondary monomer insertion.[55−57] On the side of highly isotactic samples, the $C_1$-symmetric complex **6** gives the best balance between productivity, stereoselectivity and molecular mass. The evidence is that **6** is strongly activated by $H_2$, up to a remarkable high productivity without excessive loss in molecular mass.[53] Adding hydrogen during polymerization has been used to control the molecular mass, and for highly isotactic samples produced with **6**, and low isotactic samples produced with **4**, samples with the same concentration of stereodefects ([*rr*] = 0.8% and 2.8% for catalysts **6** and **4**, respectively) and different molecular masses have been prepared (Table 1).

The microstructural characteristics of the synthesized iPB samples of Table 1 allow studying the effect of the *rr* stereodefects, of 4,1 regiodefects and of the molecular mass on the polymorphic behavior of iPB and the crystallization from the melt of the different polymorphic forms of iPB.

The X-ray powder diffraction profiles of the iPB samples of Table 1 crystallized from the melt by cooling the melt to room temperature (or at temperatures lower than the room temperature) at cooling rate of 10 °C/min, are reported in Figure 1. It is apparent that all the more stereoregular samples

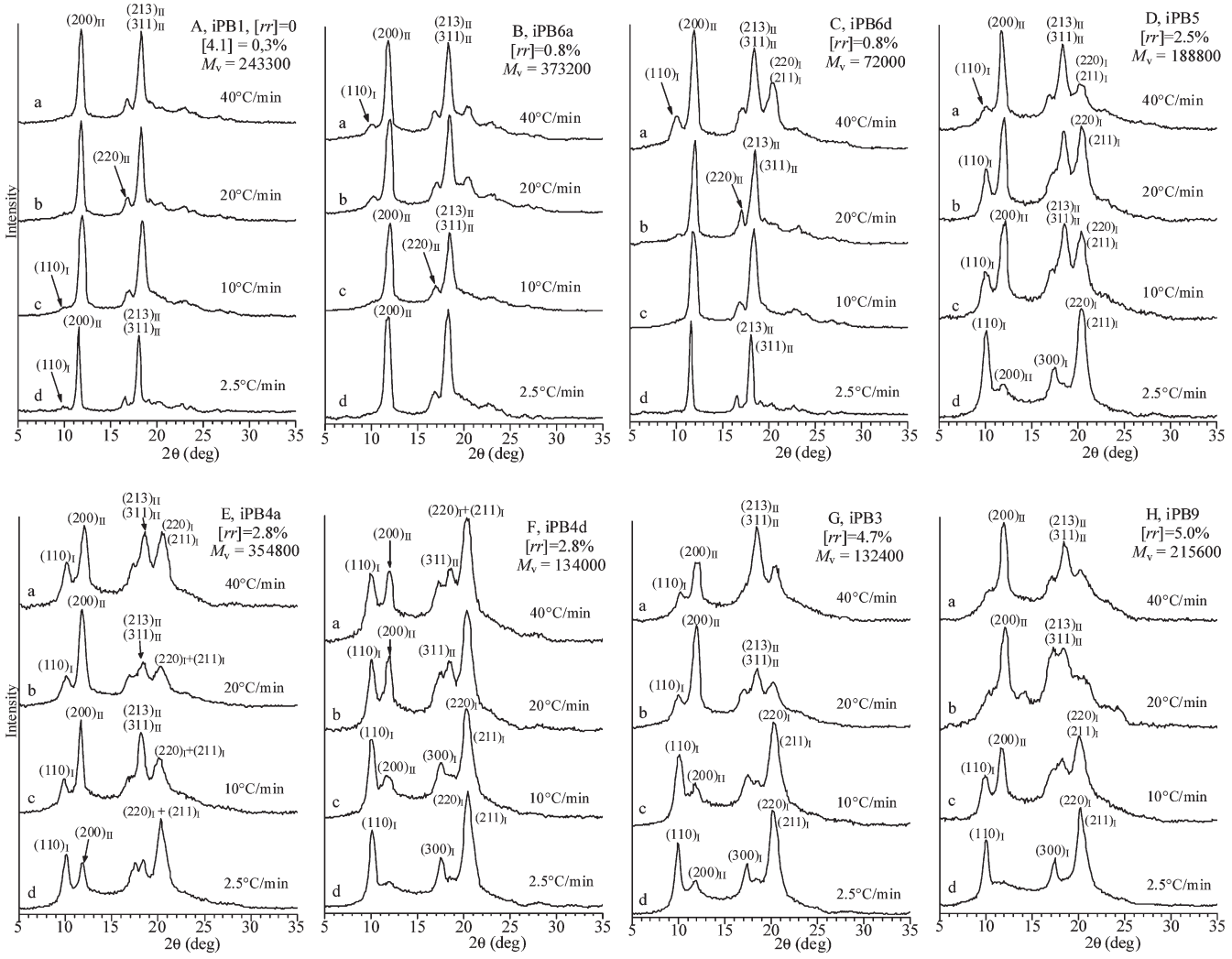


**Figure 2.** X-ray powder diffraction profiles of samples of iPB of different stereoregularity crystallized from the melt by cooling the melt to room temperature (or lower temperature) at the indicated cooling rates. The $(110)_I$, $(300)_I$, and $(220)_I + (211)_I$ reflections of form I at $2\theta = 9.9$, 17.3, and 20.5°, respectively, and the $(200)_{II}$, $(220)_{II}$, and $(213)_{II} + (311)_{II}$ reflections of form II at $2\theta = 11.9$, 16.9, and 18.3°, respectively, are indicated.

with concentration of *rr* stereodefects lower than 1.4 mol %, crystallize from the melt into form II, as indicated by the presence of the $(200)_{II}$, $(220)_{II}$, and $(213)_{II} + (311)_{II}$ reflections at $2\theta = 11.9$, 16.9, and 18.3°, respectively, in the diffraction profiles a−i of Figure 1. The crystallization of the metastable form II from the melt is the common behavior of iPB observed in samples of iPB prepared with Ziegler−Natta catalysts and extensively described in the literature.[3,6−14]

The diffraction profiles of the melt-crystallized specimens of the more stereoirregular iPB samples, with concentration of *rr* defects higher than 1.4 mol %, present, besides the $(200)_{II}$, $(220)_{II}$, and $(213)_{II} + (311)_{II}$ reflections of form II at $2\theta = 11.9$, 16.9, and 18.3°, respectively, also the $(110)_I$, $(300)_I$, and $(220)_I + (211)_I$ reflections of form I at $2\theta = 9.9$, 17.3, and 20.5°, respectively (profiles l−r of Figure 1). This indicates that the stereoirregular samples of iPB crystallize from the melt as mixtures of form II and form I. Since form I refers usually to a crystal modification that is generated via a solid-state transformation of form II by aging at room temperature, and form I′ refers to the same trigonal crystal structure obtained by direct crystallization from melt or solution,[12] the crystalline form I obtained directly from the melt in the stereoirregular iPB samples of Figure 1 (profiles l−r of Figure 1) should be, actually, defined as form I′. This is the first experimental evidence of the crystallization of the stable trigonal form I of iPB directly from the melt at atmospheric pressure. Hereinafter, the trigonal form obtained in our experiments by direct crystallization from the melt is defined form I′.

The data of Figure 1 indicate that the presence of non-negligible amount of *rr* stereodefects induces the crystallization of form I′ instead of the metastable form II. From the diffraction profiles l−r of Figure 1, it can be realized that the amount of form I′ that crystallizes from the melt, along with the metastable form II, depends on the concentration of stereodefects but also on the molecular mass and the cooling rate from the melt. The X-ray powder diffraction profiles of some samples of iPB of Figure 1 crystallized from the melt at different cooling rates are reported in Figure 2. It is apparent that the most stereoregular samples crystallize from the melt always in the metastable form II at any cooling rate (Figure 2A−C). Only for samples with low molecular mass, a small amount of crystals of form I′ develops during the melt crystallization at the highest cooling rate, as demonstrated by the presence of the $(110)_I$ reflection of form I′ at $2\theta = 9.9°$ in the diffraction profile a of Figure 2C. As already shown in Figure 1 the more stereoirregular samples with concentration of *rr* stereodefects higher than 1.4 mol % crystallize from the melt as mixtures of form I′ and form II, and the data of Figure 2D-H demonstrate that the amount of form I′ increases with decreasing cooling rate. The intensities of the reflections of form I′, indeed, increase with decreasing cooling rate in the diffraction profile of Figure 2D-H. The most irregular samples

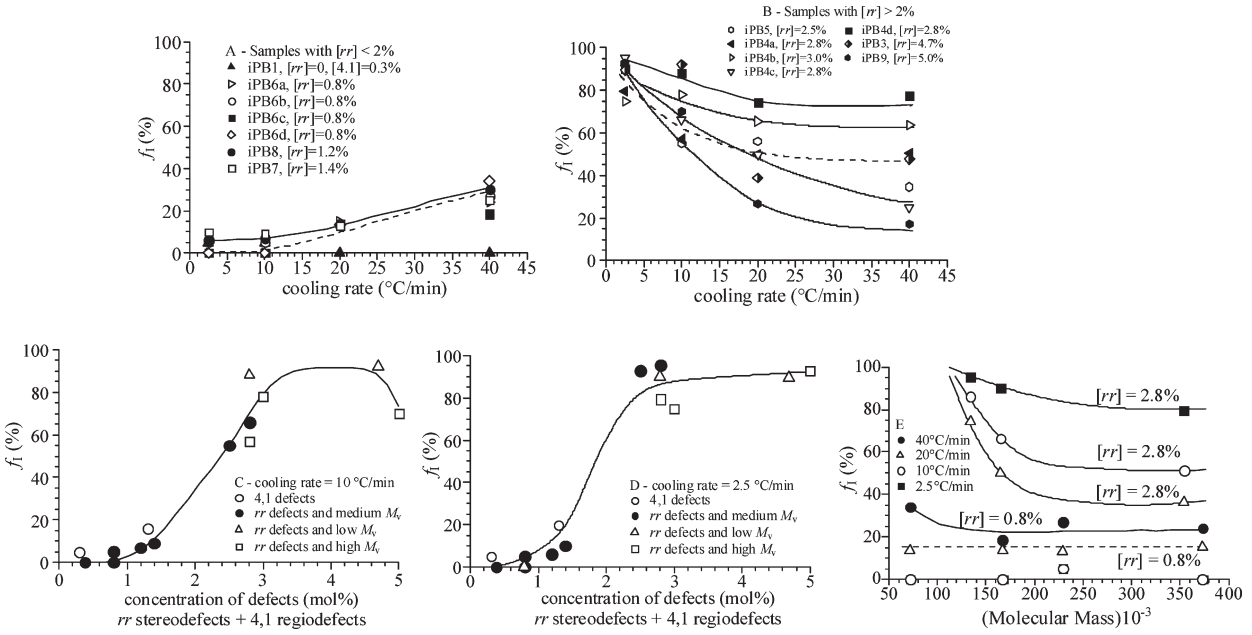


**Figure 3.** Relative amount of crystals of form I′ of iPB ($f_I$) with respect to those of form II that crystallize from the melt by cooling the melt at different cooling rates, as a function of cooling rate (A,B), for samples of iPB of different stereregularity with concentration of *rr* defects lower (A) and higher (B) than 2 mol %, as a function of the total concentration of defects (*rr* stereodefects plus 4,1-regiodefects) for iPB samples crystallized from the melt by cooling the melt at 10 °C/min (C) and 2.5 °C/min (D), and as a function of the molecular mass for samples with [*rr*] = 0.8% and 2.8% crystallized at different cooling rates (E).

iPB5, iPB 4d, iPB3 and iPB9 crystallize from the melt at cooling rate of 2.5 °C/min almost completely into form I′ (profiles d of Figure 2, parts D, F, G, and H, respectively). Only for the stereirregular sample iPB4a with high molecular mass even at low cooling rate of 2.5 °C/min does a high fraction of form II still crystallize (profile d of Figure 2E).

The relative amount of crystals of form I′, with respect to the crystals of form II, that crystallize from the melt at the different cooling rates, can be evaluated from the X-ray diffraction profiles of Figures 1 and 2 from the intensities of the $(110)_I$ reflection at $2\theta = 9.9°$ of form I′ and the $(200)_{II}$ reflection at $2\theta = 11.9°$ of form II. The fraction of crystals of form I′ for the iPB samples of different stereoregularity crystallized from the melt is reported in Figure 3 as a function of the cooling rate (Figure 3A,B) and of the total concentration of microstructural defects (*rr* streredefects and 4,1 regiodefects) (Figure 3C,D). It is apparent that for samples with concentration of defects higher than 2 mol % the concentration of crystals of form I′ increases with decreasing cooling rate (Figure 3B), and at low cooling rate (2.5 °C/min) only form I′ is obtained, whereas a small amount of form II is present only for samples of high molecular mass (samples iPB4a and iPB4b) (Figures 3B and 2E). The most regular samples, with defects concentration lower than 2 mol %, crystallize, instead, basically in the form II and a small amount of form I′ develops only by crystallization at high cooling rates, in particular for samples with low molecular mass (for instance the sample iPB6d) (Figures 3A and 2C). However for the most isotactic samples iPB1 and iPB2 with very low concentration of *rr* stereodefects ([*rr*] = 0 and 0.34%, respectively) containing non negligible amount of regiodefects (0.3% and 0.96% of 4,1 units, respectively), a small amount of crystals of form I′ (about 5%) crystallizes at low cooling rates (Figures 2A and 3A), as indicates by the presence of the $(110)_I$ at $2\theta = 9.9°$ of low intensity in the diffraction profiles a,b of Figure 1 and profiles c,d of Figure 2A. Moreover, the data of Figure 3C and D clearly indicate that for crystallizations from the melt at cooling rates of 10 and 2.5 °C/min, the amount of crystals of form I′ increases with increasing the concentration of microstructural defects (*rr* stereodefects and 4,1 regiodefects), up to a crystallization of the pure form I′ form the melt in the most irregular samples by slow crystallization at 2.5 °C/min (Figure 3D). Furthermore, it is apparent in Figure 3C,D that at the same total concentration of defects, samples containing 4,1 regiodefects (iPB1 and iPB2) show higher amount of form I.

All the data of Figures 1−3 indicate that the direct crystallization of form I′ from the melt seems to be favored by high concentration of *rr stereo*-defects and 4,1 *regio*-defects, a low crystallization rate, and a low molecular mass. The influence of the molecular mass on the crystallization from the melt of forms I and II for stereoregular and stereoirregular samples can be understood through the analysis of the crystallization behavior of the highly isotactic samples iPB6a−iPB6d prepared with the isospecific catalyst **6** and showing different molecular masses, and of the stereirregular samples iPB4a−iPB4d, prepared with the less isospecific catalyst **4** (Table 1). The fraction of form I′ for the iPB samples of different molecular mass crystallized from the melt at different cooling rates is reported in Figure 3E as a function of the molecular mass. As shown in Figure 2, the more isotactic samples with [*rr*] = 0.8% crystallize basically in form II ($f_I \approx 0$) at low cooling rates of 2.5 and 10 °C/min regardless of the molecular mass, and small fractions of crystals of form I′ develop at higher cooling rate. At the highest cooling rate (40 °C/min) the fraction of form I′ slightly increases with decreasing molecular mass (Figure 3E). For the low stereoregular samples with [*rr*] = 2.8%, instead, the fraction of form I′ increases with decreasing molecular mass at any cooling rate.

To demonstrate that in stereodefective iPB samples crystals of form I′ are obtained directly from the melt and not from rapid transformation of crystals of form II obtained from the melt, experiments of time resolving X-ray diffraction during isothermal melt-crystallization have been performed. Samples of iPB have been isothermally crystallized at different temperatures and the X-ray diffraction profiles have been recorded at the crystallization temperature during the crystallization. Since the reflections diagnostic of crystals of form I and form II are in the range of the diffraction angle $2\theta = 9-13°$ ($(110)_I$ reflection of form I at

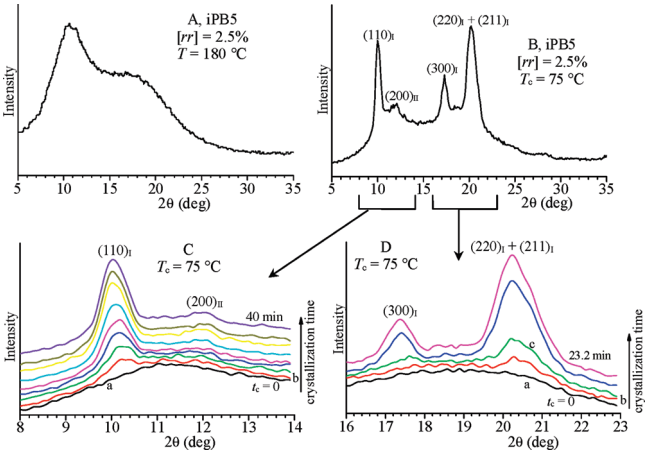


**Figure 4.** X-ray powder diffraction profiles of the sample iPB5 with [*rr*] = 2.5 mol % recorded at 180 °C (A) (melted sample), and at the crystallization temperature of 75 °C during the isothermal melt-crystallization (C,D) and of the sample completely crystallized at 75 °C (B). The $(hkl)_I$ reflections of form I′ at $2\theta$=9.9, 17.3, and 20.5° and the $(200)_{II}$ reflection of form II at $2\theta$ = 11.9°, are indicated. In parts C and D the diffraction profiles are recorded at the crystallization time $t_c$ = 0, 5, 10, 15, 20, 25, 30, 35, and 40 min (C), and $t_c$ = 0, 5.8, 11.6, 17.4, and 23.2 min (D).

$2\theta$=9.9° and $(200)_{II}$ reflection of form II at $2\theta$=11.9°), and in the range of $2\theta$ = 16−22° ($(300)_I$ and $(220)_I$ + $(211)_I$ reflections of form I at $2\theta$ = 17.3 and 20.5°, and $(213)_{II}$ + $(311)_{II}$ reflections of form II at $2\theta$ = 18.3°), the diffraction profiles have been recorded during the isothermal crystallization only in the ranges of $2\theta$ = 8−14° and $2\theta$ = 16−23°. Each sample has been first heated at 180 °C and completely melted and the diffraction profile of the melt has been recorded at 180 °C. Then the samples have been rapidly cooled to the crystallization temperature $T_c$ and the diffraction profiles have been recorded with continuous scans at collecting rate of 1.2 degree/min, so that the $2\theta$ range 8−14° is recorded in 5 min, whereas the $2\theta$ range 16−23° is collected in 5.8 min. Successive diffraction profiles are collected every 5 min in the range $2\theta$=8−14° and every 5.8 min in the range $2\theta$=16−23°, up to the complete crystallization at $T_c$.

The experiments of isothermal crystallization of the stereo-defective sample iPB5 with concentration of *rr* defects of 2.5% at the crystallization temperature $T_c$=75 °C are reported in Figure 4. The X-ray diffraction profile of the melted sample recorded at 180 °C is reported in Figure 4A, the diffraction profiles recorded at the crystallization temperature $T_c$ = 75 °C are shown in Figure 4C,D and the diffraction profile of the sample completely crystallized at 75 °C is reported in Figure 4B.

The sample iPB5 crystallizes at $T_c$=75 °C almost completely in the form I, as indicated by the diffraction profile of the sample completely crystallized at 75 °C of Figure 4B that presents mostly the reflections of form I′ at $2\theta$ = 9.9, 17.3 and 20.5°, and only a small peak at $2\theta$=11.9°, corresponding to the $(200)_{II}$ reflection of form II. The final fraction of form I′ at the end of the isothermal crystallization is 94%. The diffraction profiles recorded at 75 °C during the crystallization at 75 °C of Figure 4C,D clearly show that, starting from the amorphous halo of the melt (profiles a of Figure 4C,D), the $(110)_I$, $(300)_I$, and $(220)_I$ + $(211)_I$ reflections of form I′ at $2\theta$ = 9.9, 17.3, and 20.5° appear at the beginning of the crystallization (profiles b of Figure 4C,D and c of Figure 4D), when no reflections of form II are observed. The intensities of the reflections of form I′ increase during the crystallization and the small peak corresponding to the $(200)_{II}$ reflection of form II at $2\theta$ = 11.9° appears only when most of form I′ has already crystallized, after about 30 min from the beginning of the crystallization. These data clearly indicate that for the stereirregular

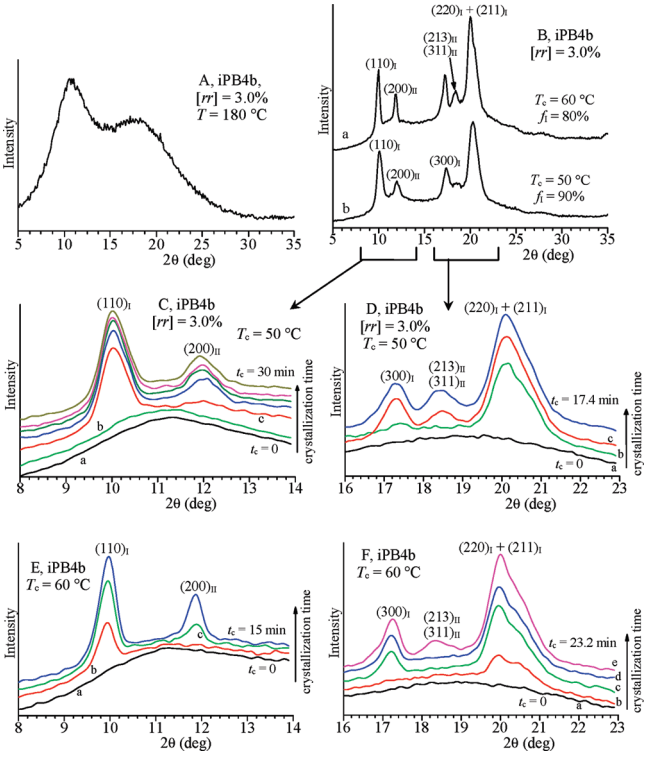


**Figure 5.** X-ray powder diffraction profiles of the sample iPB4b with [*rr*] = 3.0 mol % recorded at 180 °C (A) (melted sample), and at the crystallization temperatures of 50 (C,D) and 60 °C (E,F) during the isothermal melt-crystallization and of the samples completely crystallized at 50 and 60 °C (B). The $(hkl)_I$ reflections of form I′ at $2\theta$ = 9.9, 17.3 and 20.5°, and the $(hkl)_{II}$ reflections of form II at $2\theta$ = 11.9, 16.9, and 18.3° are indicated. In parts C−F, the diffraction profiles are recorded at the crystallization time $t_c$ = 0, 5, 10, 15, 20, 25, and 30 min (C), $t_c$ = 0, 5.8, 11.6, and 17.4 min (D), $t_c$ = 0, 5, 10, and 15 min (E), and $t_c$ = 0, 5.8, 11.6, 17.4, and 23.2 min (F).

sample iPB5 crystals of form I′ are obtained directly from the crystallization from the melt. The hypothesis that crystals of form I could be obtained from the rapid transformation by aging at room temperature of the crystals of form II formed from the melt-crystallization may be, therefore, ruled out.

Similar experiments have been performed for the other stereo-defective samples iPB4a−iPB4d, iPB3, and iPB9. Two examples of isothermal melt-crystallizations that produce mixtures of crystals of form I′ and form II are shown in Figure 5. The X-ray diffraction profile of the stereirregular sample iPB4b, with [*rr*] = 3.0%, recorded at 180 °C is reported in Figure 5A, the diffraction profiles recorded at the crystallization temperatures $T_c$=50 and 60 °C are shown in Figure 5C−F, and the diffraction profiles of the sample completely crystallized at 50 and 60 °C are reported in Figure 5B. It is apparent that the sample iPB4b is in the melt state at 180 °C (Figure 5A) and crystallize isothermally at 50 and 60 °C as mixtures of crystals of form I′ and form II (Figure 5B), the fractions of crystals of form I′ are 80 and 90% at $T_c$ = 60 and 50 °C, respectively (Figure 5B).

The diffraction profiles recorded at 50 and 60 °C during the isothermal crystallizations of the sample iPB4b show that, starting from the amorphous halo of the melt (profiles a of Figure 5C−F), the reflections of form I′ at $2\theta$ = 9.9, 17.3, and 20.5° appear at the beginning of the crystallization (profiles b of Figure 5C−F), whereas the reflections of form II at $2\theta$ = 11.9 and 18.3°, are still absent. The intensities of the reflections of form I′ increase during the crystallization and the $(200)_{II}$, $(213)_{II}$, and $(311)_{II}$ reflections of form II appear only at longer crystallization time, at least after 10−15 min from the beginning of the

crystallization (profile c of Figure 5C,D,E and profile e of Figure 5F), when most of form I′ has already crystallized. The data of Figure 5 clearly indicate that even when the crystallization form the melt produces a mixture of crystals of form I′ and form II, form I′ is obtained directly from the melt and not from the rapid transformation by aging at room temperature of the crystals of form II formed from the melt-crystallization. In particular, for the stereodefective sample iPB4b, crystals of form I′ are first obtained at beginning of the crystallization, whereas form II crystallizes later at longer crystallization times.

These data indicate that iPB may crystallize from the melt into the stable form I′ in stereodefective samples, when the concentration of stereodefects is higher than about 2 mol %. The data of Figures 1−5 represent the first experimental evidence of the crystallization of the stable trigonal form I′ of iPB directly from the melt in bulk samples at atmospheric pressure. To date direct crystallization at atmospheric pressure of form I′ of iPB from the melt has been obtained only by self-nucleation,[33] or epitaxy,[30] or in single crystals in ultrathin films.[34] The presence of *rr* stereodefects, therefore, favors the crystallization from the melt of the stable form I′ over that of the form II, which is the kinetically favored modification in highly isotactic samples. This is probably due to the fact that the presence of *rr* defects increases the flexibility of the chains, making the crystallization kinetics of form I in non isothermal conditions competitive with that of form II. Moreover, the presence of high concentration of *rr* defects also produces a decrease of the thermodynamic stability of form II, through the reduced stability of the 11/3 helical conformation of form II, compared to the 3/1 helical conformation of form I. The effect of the presence of *rr* defects, is, probably, similar to that of the incorporation of comonomeric units in isotactic copolymers of 1-butene with α-olefins having a number of carbon atom less than five, which induces a reduced stability of the 11/3 helical conformation of form II compared to the 3/1 helical conformation of form I.[5] This reduced stability of the 11/3 helices increases the rate of transformation at room temperature of form II into form I in the case of copolymers,[5,58] and, probably, also the crystallization kinetics of form I from the melt increases. As shown by Alfonso et al.,[58] indeed, in the case of isotactic copolymers of 1-butene with ethylene, a nonnegligible fraction of low-melting form I crystals were already present in samples obtained by compression-molding at 180 °C and subsequent quenching in cold water. These crystals could be either generated in the early stages of transformation[58] of form II or also formed directly from the melt.

On the other hand, as shown in Figure 4 and 5, the fact that during the isothermal crystallizations form I′ crystallizes first and form II crystallize later at longer crystallization times, indicates that the crystallization kinetics of form I′ becomes competitive with that of form II. This is also because the induction time for primary crystallization of form II becomes higher than that of form I′ in the presence of stereodefects. In fact, the reduced stability of the 11/3 helical conformation with respect to the 3/1 helical conformation is expected to have large influence on the height of barrier for formation of nuclei of form II.

The effects of the molecular mass and of the cooling rate on the crystallization of form I, shown in Figure 3, can be also explained on the basis of these thermodynamic and kinetic factors. The experimental data of Figure 3, parts A, B, and E, can be, indeed, analyzed in the framework of current theories of crystallization kinetics.[59] Concerning the effect of the molecular mass for stereoirregular samples ([*rr*] = 2.8%), the observation of Figure 3E that the relative amount of form I′ increases with decreasing molecular mass, could be easily explained with the increase of the chain mobility with decreasing molecular mass, making the crystallization kinetics of form I′ in non isothermal conditions competitive with that of form II. This kinetic effect is appreciable only for stereoirregular samples where the high concentration of *rr* defects produces decrease of the thermodynamic stability of form II, because of the reduced stability of the 11/3 helix. When the concentration of stereodefects is low ([*rr*] = 0.8%), instead, form II remains sufficiently stable so that the kinetic effect of the low molecular mass is not appreciable and the amount of form I′ is very low even at the lowest molecular mass.

Similar balance between thermodynamic and kinetic effects can be invoked to explain the experimental observation that the amount of form I′ increases with decreasing cooling rate for stereodefective samples with [*rr*] > 2 mol % (Figure 3B). In fact, since in stereodefective samples with [*rr*] > 2 mol % the presence of *rr* defects produces decrease of stability of form II, and the kinetics of crystallization of the two forms becomes competitive with an increase of the induction time for primary crystallization of form II, at low crystallization rates (low cooling rates) the more stable form I′ is favored and almost a pure form I′ crystallize from the melt at low cooling rates in samples with *rr* defects in the concentration range 2.5−5 mol % (Figure 2 and 3B). For the same stereoirregular samples the amount of crystallized form II increases with increasing cooling rate and only for the samples with low molecular mass high concentration of form I′ is still observed at high cooling rate (sample iPB4d in Figure 3B). This indicates that even for high concentration of *rr* defects, at high cooling rates and high molecular mass, form II is still slightly kinetically favored. At low cooling rates, the much higher thermodynamic stability of form I′ in the presence of *rr* defects prevails over the higher crystallization rate of form II, and the crystallization of form I′ prevails.

The last experimental observation that for stereoregular samples with [*rr*] ≈ 0.8% the amount of form I′ increases with increasing cooling rate (Figure 3A), in particular for the sample with low molecular mass iPB6d (Figure 2C), is more difficult to explain. As mentioned above, when the concentration of stereodefects is low ([*rr*] < 2 mol %) form II remains sufficiently stable and should be still kinetically favored. These samples, indeed, crystallize basically in form II at any cooling rate, and the amount of form I′ that is observed after crystallization by cooling the melt is quite low ( < 30%), even at large cooling rate (Figure 2 and 3A). In this cases, indeed, the effect of cooling rates may be understood considering not only the fact that the crystallization of these sample is the result of the balance between thermodynamic and kinetic effects, but also the fact that the relative amount of form I/form II able to crystallize from the melt at a given temperature $T_c$, depends on the relative number of active nuclei which are formed by cooling the melt up to $T_c$. To analyze this point the crystallization temperatures of all samples have been evaluated from the DSC cooling curves from the melt and the values of the minimum lamellar thickness have been evaluated from the crystallization temperatures by application of the Lauritzen−Hoffman nucleation theory.[59]

The values of the crystallization temperatures of iPB samples measured in DSC scans at cooling rates of 2.5, 10, 20, and 40 °C/min, are reported in Figure 6A as a function of the total concentration of defects. Of course, for each sample (at fixed defect concentration) the higher the cooling rate, the lower the crystallization temperature and the higher the undercooling. At a fixed cooling rate the crystallization temperature decreases with increasing concentration of defects. In particular, for iPB samples with a concentration of defects lower than 1.4 mol %, crystallization takes place at temperatures comprised in the range 50−80 °C, whereas samples with defect content higher than 3 mol % crystallize at temperatures lower than ≈50 °C.

According to Lauritzen-Hoffman nucleation theory[59] the nuclei of a crystalline form that may become active at a given undercooling $\Delta T = T_m^0 - T_c$, with $T_m^0$ the equilibrium melting temperature of the crystal phase, should be characterized by

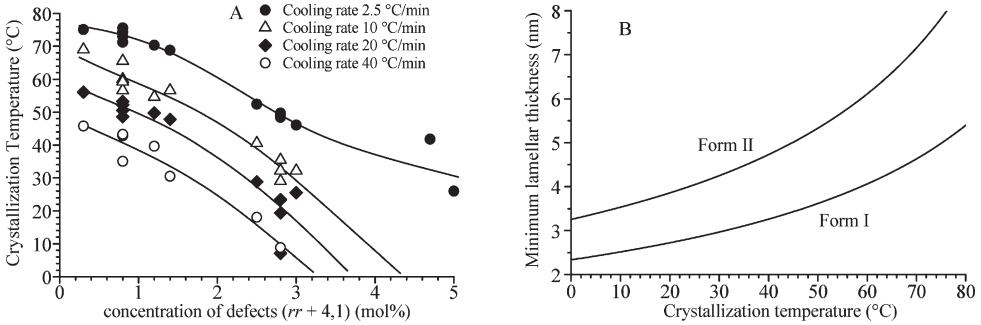


**Figure 6.** (A) Crystallization temperatures as a function of the total concentration of defects, evaluated from DSC curves at cooling rates of 2.5 °C/min (●), 10 °C/min (△), 20 °C/min (♦), and 40 °C/min (○). (B) Minimum thickness required for the lamellar crystals of form I and form II to grow as a function of crystallization temperature (eq 1).

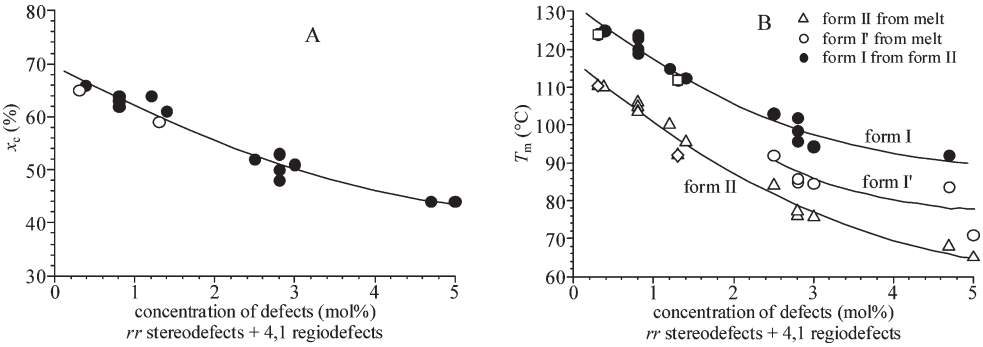


**Figure 7.** (A) Degree of crystallinity of samples crystallized from the melt by cooling the melt to room temperature at 10 °C/min, evaluated form the X-ray diffraction profiles of Figure 1, as a function of the total concentration of defects (*rr* stereodefect plus 4,1 regiodefects). (B) Melting temperatures as a function of the total concentration of defects, measured from DSC scans at heating rate of 10 °C/min, of crystals of form II (△) and form I′ (○) of iPB samples crystallized from the melt by cooling the melt to room temperature at 10 °C/min, and of crystals of form I (●) obtained by spontaneous transformation of form II (obtained by crystallization from the melt by cooling the melt to room temperature at 10 °C/min) by aging the melt-crystallized samples at room temperature for long time. Samples with defect concentration lower than 2 mol % crystallize from the melt only in form II and only the melting temperature of crystals of form II (△) are reported. Samples with defect content higher than 2 mol % crystallize from the melt as mixtures of form I′ and form II and for each sample the two melting temperatures of form II (△) and form I′ (○) are reported. The melting temperatures (◇, □) and crystallinity (○) of samples iPB1 and iPB2 containing 4,1 regiodefects are indicated with different symbols.

thicknesses higher than a minimum value $l_{min}$, which is given by the Gibbs−Thomson relation:[60]

$$l_{\min} = \frac{2\sigma_e T_m{}^0}{\Delta h_m \Delta T} \quad (1)$$

In eq 1, $\Delta h_m$ is the melting enthalpy per unit volume of the crystal phase and $\sigma_e$ is the end-surface free energy per unit area of polymer crystals. The lower the minimum lamellar thickness at a given $\Delta T$, the higher the number of active nuclei able to trigger crystallization of a given crystalline form. The minimum lamellar thickness $l_{min}$ of form I′ and form II of iPB have been calculated as a function of crystallization temperature, by setting the values of the parameters $T_m{}^0$, $\Delta h_m$ and $\sigma_e$ of eq 1 equal to 142 °C, $1.35\times10^8$ J m$^{-3}$ and $53.9\times10^{-3}$ J m$^{-2}$ respectively for form I and 129.4 °C, $1.09\times10^8$ J m$^{-3}$ and $57\times10^{-3}$ J m$^{-2}$ for form II.[33] The values of $l_{min}$ are reported in Figure 6B as a function of the crystallization temperature. It is apparent that $l_{min}$ decreases with decreasing $T_c$ (increasing undercooling, increasing cooling rate), and that the minimum thickness required for the lamellar crystals to grow is lower for form I′ than for form II.

This indicates that the kinetic restraints for obtaining nuclei able to grow crystals are less demanding for form I than for form II. The fact that in highly stereoregular iPB samples in the normal crystallization conditions form I is not obtained directly from the melt, and only form II crystallizes is due to the fact that in these samples the crystallization rate of form II largely exceeds that of form I. In fact, the growth rate of form I crystals in highly stereoregular iPBs is ≈1/100 that of form II crystals.[33]

Only when the crystallization rate of form I is not too low, a number of active nuclei of form I may be formed upon cooling the melt. In the case of stereoregular iPB samples with concentration of *rr* defects in the range 0.8−1.4 mol %, which at low cooling rates crystallize essentially in form II (Figure 1 and 3A), indeed, it is possible that these concentrations of stereodefects are enough to increase chain flexibility and improve the crystallization kinetics of form I, so that a nonnegligible number of nuclei of thickness higher than $l_{min}$ able to grow crystals of form I may be formed during cooling. Since the number of active nuclei is expected to increase with decreasing $T_c$ ($l_{min}$ decreases with decreasing $T_c$, Figure 6B), and the crystallization temperature decreases with increasing the cooling rate (Figure 6A), for these samples the amount of form I′ crystals also increases with increasing the cooling rate. In other terms, this morphological effect can influence the relative amount of form I/form II crystals, which can be obtained from the melt, only if, for some mechanism, i.e., the presence of randomly distributed stereodefects along the chain in our case, the relative stability of form II decreases, and the kinetics of crystallization of the two forms becomes competitive.

The morphological effect may be invoked also to explain the fact that the relative amount of form I′ decreases, and, therefore, that the content of form II increases with increasing cooling rate in stereoirregular iPB samples with concentration of defects higher than 2 mol % (Figure 3B). As explained above, these samples, crystallize from the melt almost completely in a pure form I′ at low cooling rate (Figure 3B). Since form II is still kinetically favored, a number of nuclei of thickness higher than

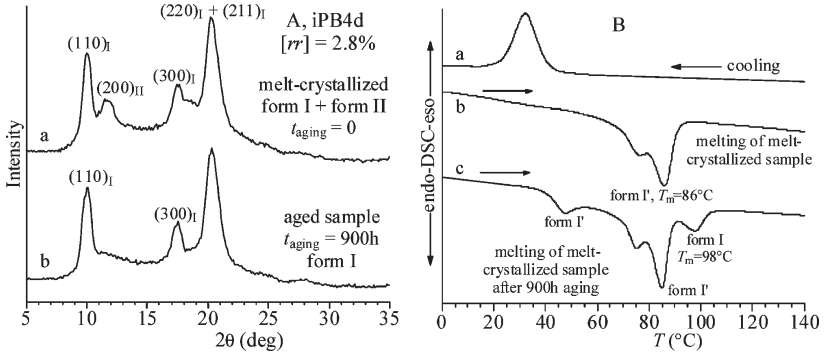


**Figure 8.** (A) X-ray powder diffraction profiles of the sample iPB4d with [*rr*] = 2.8%, crystallized from the melt by cooling the melt to room temperature at cooling rate of 10 °C/min (a), as in the DSC cooling curve a, and of the same melt-crystallized sample after aging at room temperature for 900 h (b). (B) DSC cooling curve from the melt at cooling rate of 10 °C/min of the sample iPB4d (a), successive DSC melting curve at heating rate of 10 °C/min of the sample iPB4d crystallized from the melt in the scan a (b) and DSC melting curve of the same melt-crystallized sample after aging at room temperature for 900 h (c).

$l_{min}$ able to grow crystals of form II also forms during cooling. Also in this case the number of active nuclei increases with decreasing $T_c$ ($l_{min}$ decreases with decreasing $T_c$, Figure 6B). Since the crystallization temperature decreases with increasing the cooling rate (Figure 6A), the amount of form II crystals should increase with increasing the cooling rate.

The diffraction profiles of Figures 1 and 2 also indicate that in the stereodefective samples that crystallize form the melt in form I′, the degree of crystallinity is not negligible. The degree of crystallinity of the samples crystallized from the melt at cooling rate of 10 °C/min, evaluated from the X-ray powder diffraction profiles of Figure 1, is reported in Figure 7A as a function of the defect concentration. It is apparent that the crystallinity decreases with increasing *rr* content but a remarkable value of 40−50% is still observed for the more irregular samples.

A further evidence of the crystallization of form I′ directly from the melt in stereodefective iPB samples is provided by the observation that for each sample the melting temperature of the crystals of form I′, obtained by direct crystallization from the melt, is always lower than the melting temperature of the crystals of form I obtained by spontaneous transformation of form II, obtained from the melt crystallization, into form I by aging the melt-crystallized sample at room temperature (Figure 7B).

An example is shown in Figure 8, where the X-ray powder diffraction profiles and the DSC melting curves of the sample iPB4d crystallized from the melt by cooling the melt to room temperature at cooling rate of 10 °C/min and of the same melt-crystallized sample after 900 h aging at room temperature are reported. As already shown in Figures 1 and 2F, the sample iPB4d crystallize from the melt at cooling rate of 10 °C/min mostly in form I′, as indicated by the high intensity of the $(110)_I$, $(300)_I$ and $(220)_I + (211)_I$ reflections of form I′ at $2\theta = 9.9$, 17.3. and 20.5° and the lower intensity of the $(200)_{II}$ reflection of form II at $2\theta = 11.9°$ in the diffraction profile a of Figure 8A, the fraction of form I being $f_I = 90\%$. This melt-crystallized sample show a DSC melting endotherm with two melting peaks at 77 and 86 °C (curve b of Figure 8B), the most intense being at the highest melting temperature of 86 °C. It is reasonable to assume that the peak at 86 °C corresponds to the melting of the crystals of form I′ produced by the melt-crystallization, which correspond to 90% of the formed crystals (profile a of Figure 8A). The melting of the fraction of crystals of form II (10%) is probably buried by the melting peaks of the form I′.

The crystals of form II in the melt-crystallized sample spontaneously transform into form I by aging at room temperature. The X-ray diffraction profile and the DSC melting curve of the melt-crystallized sample after aging at room temperature for 900 h are also reported in Figure 8. In the diffraction profile the $(200)_{II}$ reflection of form II at $2\theta = 11.9°$ disappears (profile b of Figure 8A), indicating that the aged sample is in the pure form I, the small fraction of crystals of form II (10%) being transformed into form I. The DSC melting curve of the aged sample still presents the melting peaks at 77 and 86 °C (curve c of Figure 8B), which, therefore, cannot be attribute to the melting of the crystals of form II, but correspond to the melting of form I′ that, indeed, does not transform by aging. Two new melting peaks appears in the DSC scan of the aged samples, one at low temperature of 45−50 °C and the second at higher temperature of 98 °C (curve c of Figure 8B). The peak at the highest temperature of 98 °C corresponds to the melting of the crystals of form I obtained by the transformation of form II by aging at room temperature (curve c of Figure 8B). The peak at the lowest temperature corresponds to the melting of defective crystals of form I′ that are probably obtained by further crystallization of the amorphous phase during the aging at room temperature.

According to the DSC data, the crystals of form I obtained by transformation of form II melt at temperature of 98 °C, higher than that of the crystals of form I′ formed by direct crystallization from the melt (86 °C) (curve c of Figure 8B). The difference in the melting temperatures of form I and form I′ has already been observed in the literature.[12] Since they show the same crystal structure,[12] form I′ has been regarded to be an imperfect form I with many defects.[27]

The DSC data of Figure 8B, in particular the fact that the area of the peaks at 77 and 86 °C corresponding to the melting of crystals obtained by melt-crystallization (curve b of Figure 8B) do not decrease after aging, confirm that these peaks correspond to the melting of the crystals of form I′ and that form I′ is obtained by direct crystallization from the melt. Moreover, the absence in the DSC curve b of Figure 8B of melting peaks whose area decrease after aging confirms that the melting peak of the small fraction of form II present in the melt-crystallized sample is buried by the melting peaks of the form I′. Therefore, in this stereodefective sample of iPB crystals of form II melt at temperature very close to the melting temperature of the crystals of form I′.

DSC data similar to those of Figure 8B have been obtained for all samples of Table 1. In some cases the melting peaks corresponding to the melting of crystals of form II and form I′, obtained from the melt, are both visible. These data have allowed for the determination of the melting temperatures of form II, form I′ and form I, the latter from the DSC melting curves of the aged samples. For all samples, as in Figure 8B, the melting temperatures of form I′ is lower than the melting temperature of crystals of form I obtained from the transformation of form II at room temperature. The melting temperatures of crystals of form

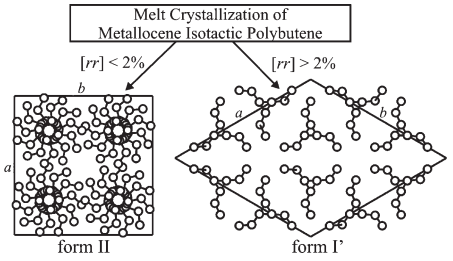


**Figure 9.** Scheme of the polymorphic behavior of metallocene made iPB that depends on the concentration of *rr* stereodefects. Stereoregular samples crystallize from the melt in the usual form II, whereas stereodefective iPB samples crystallize from the melt in the trigonal form I′.

II and form I′ obtained by direct crystallization from the melt by cooling the melt to room temperature at 10 °C/min, and of crystals of form I, obtained by the spontaneous transformation of form II at room temperature, are reported for all iPB samples in Table 1 and in Figure 7B as a function of the total concentration of defects (*rr* stereodefect plus 4,1 regiodefects). It is apparent that the melting temperatures of all crystals (form I′, form II, and form I) decrease with increasing concentration of defects, and the melting temperature of form I is always higher than those of form I′ and form II. Moreover the melting temperature of form I′ is slightly higher than that of form II.

## Conclusions

Samples of isotactic polybutene of different stereoregularity, containing different concentrations of stereodefects (*rr* triads defects) and regiodefects (4,1 units) have been prepared with different $C_2$- and $C_1$-symmetric metallocene catalysts. The concentration of *rr* stereodefects has been tailored through the choice of the ligand structure of the highly regiospecific $C_1$-symmetric catalysts.

A study of the crystallization from the melt and of the polymorphic behavior of the iPB samples of different stereoregularity is presented. The main result is summarized in Figure 9. Highly isotactic samples, with concentration of *rr* stereodefects lower than 2 mol %, crystallize from the melt in the metastable form II. This is a common polymorphic behavior observed in iPB samples prepared with Ziegler−Natta catalysts and extensively reported in the literature. A higher concentration of *rr* defects produces direct crystallization from the melt of form I′. In fact, stereodefective iPB samples with *rr* content higher than 2 mol %, crystallize form the melt as mixtures of form II and form I′, the fraction of crystals of form I′ increases with increasing concentration of defects, decreasing cooling rate from the melt and decreasing the molecular mass. Samples with concentration of *rr* defects of 3−4 mol % crystallize from the melt in the pure form I′ at low cooling rates. The direct crystallization of form I′ from the melt seems to be favored by high concentration of *rr stereo*-defects and 4,1 *regio*-defects, low crystallization rate and low molecular mass.

Crystals of form I′ formed by direct melt-crystallization melt at temperatures lower than that of crystals of form I obtained by transformation of form II at room temperature. Since form I and form I′ show the same crystal structure, form I′ has been regarded to be an imperfect form I with many defects.

The results reported in this paper provide the first experimental observation of the crystallization of the stable trigonal form I′ of iPB from the melt at atmospheric pressure. This result may be of interest because the crystallization of the metastable form II from the melt and the spontaneous transformation at room temperature of form II into the stable form I has been considered for long time an unavoidable problem that stands in the way of the industrial development of the Ziegler−Natta iPB.

**Acknowledgment.** Financial supports from Basell Polyolefins (Ferrara, Italy) and from the "Ministero dell'Istruzione, dell'Università e della Ricerca" (PRIN 2007 project) are gratefully acknowledged.

## References and Notes

(1) Natta, G.; Pino, P.; Corradini, P.; Danusso, F.; Mantica, E.; Mazzanti, G.; Moraglio, G. *J. Am. Chem. Soc.* **1955**, *77*, 1708–1710.
(2) Natta, G.; Corradini, P.; Bassi, I. W. *Nuovo Cimento* (*Suppl.*) **1960**, *15*, 52–67.
(3) Natta, G.; Corradini, P.; Bassi, I. W. *Makromol. Chem* **1956**, *21*, 240.
(4) Turner-Jones, A. *J. Polym. Sci., Part B* **1963**, *1*, 455.
(5) Turner-Jones, A. *Polymer* **1966**, *7*, 23. Turner-Jones, A. *J. Polym. Sci., Part B* **1965**, *3*, 591.
(6) Petraccone, V.; Pirozzi, B.; Frasci, A.; Corradini, P. *Eur. Polym. J.* **1976**, *12*, 323.
(7) Corradini, P.; Napolitano, R.; Petraccone, V.; Pirozzi, B. *Eur. Polym. J.* **1984**, *20*, 931.
(8) Cojazzi, G.; Malta, V.; Celotti, G.; Zannetti, R. *Makromol. Chem.* **1976**, *177*, 915.
(9) Dorset, D. L.; McCourt, M. P.; Kopp, S.; Wittmann, J. C.; Lotz, B. *Acta Crystallogr.* **1994**, *B50*, 201.
(10) Lotz, B.; Thierry, A. *Macromolecules* **2003**, *36*, 286–290.
(11) Luciani, L.; Seppälä, J.; Löfgren, B. *Prog. Polym. Sci.* **1988**, *13*, 37–62.
(12) Holland, V. F.; Miller, R. L. *J. Appl. Phys.* **1964**, *35*, 3241.
(13) Chau, K. W.; Geil, P. H. *J. Macromol. Sci. Phys.* **1984**, *B23*, 115.
(14) Tosaka, M.; Kamijo, T.; Tsuji, M.; Kohjiya, S.; Ogawa, T.; Isoda, S.; Kobayashi, T. *Macromolecules* **2000**, *33*, 9666.
(15) Boor, J., Jr.; Mitchell, J. C. *J. Polym. Sci.: Part A* **1963**, *1*, 59.
(16) Powers, J.; Hoffman, J. D.; Weeks, J. J.; Quinn, F. A. Jr. *J. Res. Natl. Bur. Stand* **1965**, *69A*, 335.
(17) Schaffhauser, R. J. *J. Polym. Sci., Part B* **1967**, *5*, 839.
(18) Gohil, R. M.; Miles, M. J.; Petermann, J. *J. Macromol. Sci. Phys.* **1982**, *B21*, 189.
(19) Fujiwara, Y. *Polym. Bull.* **1985**, *13*, 253.
(20) Chau, K. W.; Yang, Y. C.; Geil, P. H. *J. Mater. Sci.* **1986**, *21*, 3002.
(21) Hsu, T.-C.; Geil, P. H. *Polym. Commun.* **1990**, *31*, 105.
(22) Miller, R. L.; Holland, V. F. *J. Polym. Sci., Part B* **1964**, *2*, 519.
(23) Kopp, S.; Wittmann, J. C.; Lotz, B. *J. Mater. Sci.* **1994**, *29*, 6159.
(24) Lotz, B.; Mathieu, C.; Thierry, A.; Lovinger, A. J.; De Rosa, C.; Ruiz de Ballesteros, O.; Auriemma, F. *Macromolecules* **1998**, *31*, 9253.
(25) Foglia, A. J. *J. Appl. Polym. Sci., Appl. Polym. Symp.* **1969**, *11*, 1–18.
(26) Danusso, F.; Gianotti, G. *Makromol. Chem.* **1963**, *61*, 139. Danusso, F.; Gianotti, G. *Makromol. Chem.* **1965**, *88*, 149.
(27) Boor, J., Jr.; Youngman, E. A. *J. Polym. Sci., Part B* **1964**, *2*, 903.
(28) Geil, P. H.; Chau, K. W.; Agarwal, A.; Hsu, C. C. In *Morphology of Polymers*; Sedlacek, B., Ed.; Walter de Gruyter: Berlin, 1986; pp 87−102.
(29) Chau, K. W.; Geil, P. H. *J. Macromol. Sci., Phys.* **1984**, *B23*, 115–142.
(30) Kopp, S.; Wittmann, J. C.; Lotz, B. *Polymer* **1994**, *35*, 908. Kopp, S.; Wittmann, J. C.; Lotz, B. *Polymer* **1994**, *35*, 916. Mathieu, C.; Stocker, W.; Thierry, A.; Wittmann, J. C.; Lotz, B. *Polymer* **2001**, *42*, 7033.
(31) Armeniades, C. D.; Baer, E. *J. Macromol. Sci. Phys.* **1967**, *B1*, 309.
(32) Nakafuku, C.; Miyaki, T. *Polymer* **1983**, *24*, 141.
(33) Yamashita, M.; Hoshino, A.; Kato, M. *J. Polym. Sci., B: Polym Phys.* **2007**, *45*, 684. Yamashita, M. *J. Cryst. Growth* **2007**, *310*, 1739. Yamashita, M. *J. Cryst. Growth* **2009**, *311*, 556. Yamashita, M. *J. Cryst. Growth* **2009**, 311 560.
(34) Zhang, B.; Yang, D.; Yan, S. *J. Polym. Sci., Polym. Phys.* **2002**, *40*, 2641.
(35) Azzurri, F.; Flores, A.; Alfonso, G. C.; Balta Calleja, F. J. *Macromolecules* **2002**, *35*, 9069.
(36) Azzurri, F.; Flores, A.; Alfonso, G. C.; Sics, I.; Hsiao, B. S.; Balta Calleja, F. J. *Polymer* **2003**, *44*, 1641.
(37) Alfonso, G. C.; Azzurri, F.; Castellano, M. *J. Therm. Anal. Calorim.* **2001**, *66*, 197.
(38) Kaszonyiova, M.; Rybnikar, F.; Geil, P. H. *J. Macromol. Sci. Phys.* **2004**, *B43*, 1095.
(39) Hong, K.; Spruiell, J. E. *J. Appl. Polym. Sci.* **1985**, *30*, 3163.
(40) Chau, K. W.; Yang, Y. C.; Geil, P. H. *J. Mater. Sci.* **1986**, *21*, 3002.

(41) Rubin, I. D. *J. Polym. Sci., Polym. Lett*. **1964**, *2*, 747–749.
(42) Gianotti, G.; Capizzi, A. *Makromol. Chem*. **1969**, *124*, 152.
(43) Asada, T.; Onogi, S. In *Structure and Properties of Polymer Films*; Stein, R. S., Ed.; Plenum Press: New York, 1973; Vol. *1*.
(44) Nakamura, K.; Aoike, T.; Usaka, K.; Kanamoto, T. *Macromolecules* **1999**, *32*, 4975–4982.
(45) Samon, J. M.; Schultz, J. M.; Hsiao, B. S.; Wu, J.; Khot, S. *J. Polym. Sci., Part B: Polym. Phys*. **2000**, *38*, 1872–1882.
(46) Boor, J.; Mitchell, J. C. *J. Polym. Sci*. **1962**, *62*, S70–73.
(47) Rubin, I. D. *J. Polym. Sci*. **1965**, *A3*, 3803–3813.
(48) Siegmann, A. *J. Appl. Polym. Sci*. **1982**, *27*, 1053.
(49) De Rosa, C.; Auriemma, F.; Di Capua, A.; Resconi, L.; Guidotti, S.; Camurati, I.; Nifant'ev, I. E.; Laishevtsev, I. P. *J. Am. Chem. Soc*. **2004**, *126*, 17040. De Rosa, C.; Auriemma, F. *J. Am. Chem. Soc*. **2006**, *128*, 11024. De Rosa, C.; Auriemma, F. *Lect. Notes Phys*. **2007**, *714*, 345. De Rosa, C.; Auriemma, F.; Paolillo, M.; Resconi, L.; Camurati, I. *Macromolecules* **2005**, *38*, 9143. De Rosa, C.; Auriemma, F.; Resconi, L. *Macromolecules* **2005**, *38*, 10080. De Rosa, C.; Auriemma, F.; De Lucia, G.; Resconi, L. *Polymer* **2005**, *46*, 9461. De Rosa, C.; Auriemma, F.; Perretta, C. *Macromolecules* **2004**, *37*, 6843. De Rosa, C.; Auriemma, F.; Circelli, T.; Waymouth, R. M. *Macromolecules* **2002**, *35*, 3622. Auriemma, F.; De Rosa, C. *Macromolecules* **2002**, *35*, 9057.
(50) Alamo, R. G.; Kim, M. H.; Galante, M. J.; Isasi, J. R.; Mandelkern, L. *Macromolecules* **1999**, *32*, 4050. VanderHart, D. L.; Alamo, R. G.; Nyden, M. R.; Kim, M. H.; Mandelkern, L. *Macromolecules* **2000**, *33*, 6078. Nyden, M. R.; Vanderhart, D. L.; Alamo, R. G. *Comp. Theor. Polym. Sci*. **2001**, *11*, 175. Alamo, R. G.; VanderHart, D. L.; Nyden, M. R.; Mandelkern, L. *Macromolecules* **2000**, *33*, 6094. Hosier, I. L.; Alamo, R. G.; Esteso, P.; Isasi, G. R.; Mandelkern, L. *Macromolecules* **2003**, *36*, 5623. Hosier, I. L.; Alamo, R. G.; Lin, J. S. *Polymer* **2004**, *45*, 3441. Alamo, R. G.; Ghosal, A.; Chatterjee, J.; Thompson, K. L. *Polymer* **2005**, *46*, 8774.
(51) (a) Resconi, L.; Cavallo, L.; Fait, A.; Piemontesi, F. *Chem. Rev*. **2000**, *100* ((4)), 1253. (b) Resconi, L.; Guidotti, S.; Camurati, I.; Frabetti, R.; Focante, F.; Nifant'ev, I. E.; Laishevtsev, I. P. *Macromol. Chem. Phys*. **2005**, *206*, 1405.
(52) De Rosa, C.; Auriemma, F.; Corradini, P.; Tarallo, O.; Dello Iacono, S.; Ciaccia, E.; Resconi, L. *J. Am. Chem. Soc*. **2006**, *128*, 80. De Rosa, C.; Dello Iacono, S.; Auriemma, F.; Ciaccia, E.; Resconi, L. *Macromolecules* **2006**, *39*, 6098. De Rosa, C.; Auriemma, F.; Ruiz de Ballesteros, O.; Resconi, L.; Camurati, I. *Macromolecules* **2007**, *40*, 6600. De Rosa, C.; Auriemma, F.; Ruiz de Ballesteros, O.; Resconi, L.; Camurati, I. *Chem. Mater*. **2007**, *19*, 5122. De Rosa, C.; Auriemma, F.; Ruiz de Ballesteros, O.; De Luca, D.; Resconi, L. *Macromolecules* **2008**, *41*, 2172.
(53) Resconi, L.; Camurati, I.; Malizia, F. *Macromol. Chem. Phys*. **2006**, *207*, 2257.
(54) Busico, V.; Cipullo, R.; Borriello, A. *Macromol. Rapid Commun*. **1995**, *16*, 269.
(55) Kioka, M.; Mizuno, A.; Tsutsui, T.; Kashiwa, N. in *Catalysis in Polymer Synthesis*; Vandenberg, E. J.; , Salamone, J. C.; , Eds.; *ACS Symposium Series 496*; American Chemical Society: Washington, DC, 1992; p 72.
(56) Tsutsui, T.; Kashiwa, N.; Mizuno, A. *Makromol. Chem., Rapid Commun*. **1990**, *11*, 565.
(57) Borriello, A.; Busico, V.; Cipullo, C.; Fusco, O.; Chadwick, J. C. *Macromol. Chem. Phys*. **1997**, *198*, 1257.
(58) Azzurri, F.; Alfonso, G. C.; Gómez, M. A.; Martì, M. C.; Ellis, G.; Marco, C. *Macromolecules* **2004**, *37*, 3755.
(59) Hoffman, J. D.; Davis, G. T.; Lauritzen, J. I., Jr. In *Treatise on Solid State Chemistry*; Hannay, N. B., Ed.; Plenum: New York, 1997; pp 497−614.Hoffman, J. D.; Miller, R. L. *Polymer* **1997**, *38*, 3151.
(60) Wunderlich, B. *Macromolecular Physics*; Academic Press: New York, 1980; Vol. *3*.